Trade-off evaluation and design Optimization of High efficiency Terrestrial (AM1.5) Five-junction Solar Cell using Crosslight Apsys

Haonan Wu[1,2]

[1]*Department of Materials Science and Engineering*
[2]*Micro and Nanotechnology Laboratory*
University of Illinois at Urbana-Champaign, Urbana, IL 61801, USA

(Completed 21 April 2018)

Abstract

The state-of-the-art in MJSC research focuses on exploring the available bandgap range, and balancing tradeoffs between overall efficiency and number of junctions and material systems (Difficulty & costs). TCAD software will be significant to simulate finely tuned stacks of materials until the optimal design is found, using advanced optimization method such as genetic algorithms to find the trade-offs hidden in # of junctions, material composition, doping, and thickness. Since the properties of Lattice-matched GaInP/GaInAs/Ge 3-junction cell is well demonstrated by many research groups, my focus would be on a rarely researched, difficult five-junction solar cell with four buffer layers.

I. INTRODUCTION AND MOTIVATION

The photovoltaic system has been regarded as one of the most essential green energy supplier in the next several decades for a long time, because the solar energy is the readily accessible without any external cost to the environment. However, the industry of photovoltaic is facing very serious bottleneck in cost-efficiency, and present PV systems cannot compete with traditional energy sources such as crude oil and natural gas without government subsidies.

There are two major directions of future developments. The first pathway would be developing low cost silicon based solar cells as well as CdTe thin film solar cells. Those solar cells are low in cost, but the theoretical maximum efficiency is restricted by Shockley-Queisser limit of relevant material. Also, those solar cells cannot be implemented in concentrated solar cell applications because of their limited thermal stability and poor high temperature performance. Consequently, the future development of this category would have concentrated on approaching the theoretical efficiency limit while reducing the material cost as much as possible.

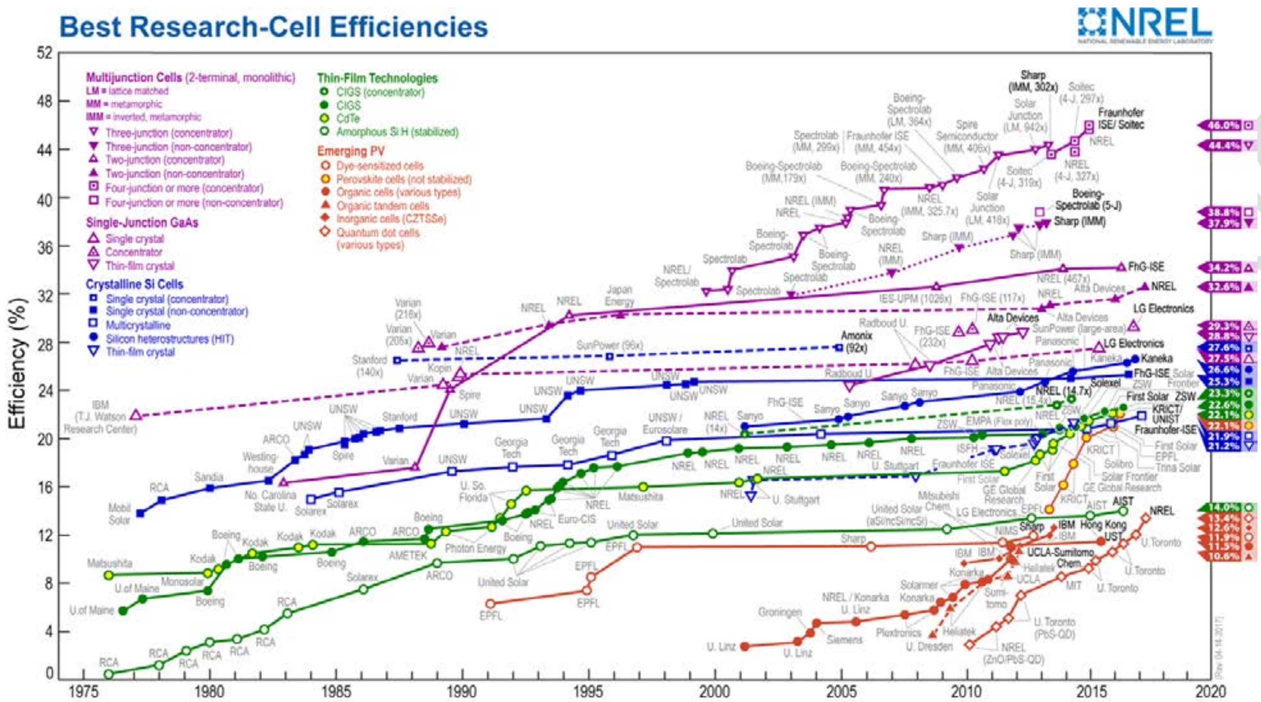

Figure 1: Present record holders of Solar cells

On the other hand, the cost efficiency could be achieved through technology that exceed the limit, in which the high cost efficiency can be obtained. Here is a list of present methods and central issues that are not yet overcome.

Table 1: Approaches to Solar Cells which exceed Shockley-Queisser limit for a single solar cell. [1]

Approach	Advantages/uses	Central Issues	Examples
Multiple spectrum	Can be implemented using low costcoatings Can use existing solar cells (or LEDs for thermophotonics)	Efficient conversion of solar spectrum not demonstrated	Thermophotovoltaic Up and down conversion
Multiple absorption	High impact ionization rates demonstrated with colloidal quantum dots Suited to conversion of high energyphotons	Transport of carriers not demonstrated	Impact ionization Two-photon absorption Raman absorption
Multiple energy level	Suited to low energy photon conversion Can capitalize on LED/photodetector devices	Demonstration of *simultaneous* radiative coupling required	Localized band (QW) Mini-band (IBSC)
Multiple temperate	Potential for high efficiencies using a single absorber material	Extraction of energy from hot carrier populations not demonstrated	Hot carriers QWs with thermal escape

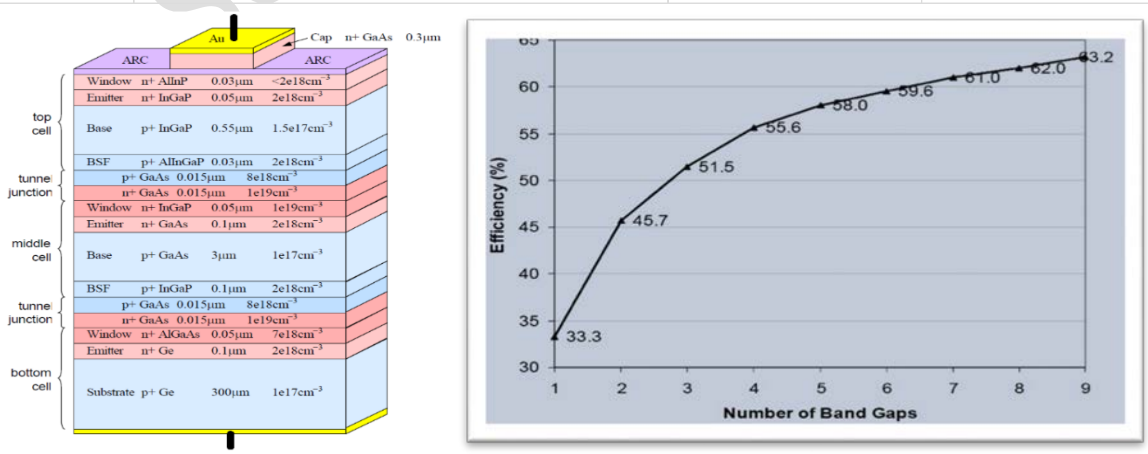

Figure 2: a) Example Triple-Junction Solar Cell. Source: [2]. b) Theoretical limit of MJSCs under AM1.5

Currently, the most practical way of achieving beyond Shockley-Queisser limit is to implement Multi-junction (MJ) solar cells. They are solar cells with multiple p–n junctions made of different semiconductor materials. Each material's p-n junction will produce electric current in response to different wavelengths of light. The use of multiple semiconducting materials allows the absorbance of a broader range of wavelengths, improving the cell's sunlight to electrical energy conversion efficiency significantly. A typical triple junction solar cell is presented in figure 2.

The state of art of this category mainly focus on improving the overall efficiency since its first application in outer-space application in the late 1970s. The greatest advantage besides its much higher overall efficiency comparing to silicon based solar cells of this category would be its great potential of concentrator PV application. It is surprising that those multi-junction solar cells will have better performance and efficiency under concentrated sunlight. It's unique and incredible feature of increasing efficiency under higher input power density opens up an entire new realm of Photovoltaic industry.

Consequently, I decided to implement a multijunction solar cell starting from an experimental baseline model and try my best to overcome all the challenges of further improving the efficiency of a baseline device. It is generally recognized that a multijunction with more than three junctions could be a nightmare to model and optimize because of extremely complex structure and current matching of so many layers. Although five and more junction solar cells have slightly increased theoretical efficiency limit [4] as figure below showed, they are rarely investigated and higher efficiency is generally harder to achieve both in numerical simulations and experiments. Below is a table of the record keeping multijunction solar cell efficiency from the 2005, and we can see that there is only one record (38.8%, Boeing Spectral Lab) for five-junction solar cell specified by the latest Research efficiency map by NREL.

Although at present stage the five-junction solar cell appears to be less efficient than those four or three junction ones, it is due to lack of research and investigation, regarding its relatively higher theoretical efficiency limit.

The lacking of research accomplishment and attention on five-junction solar cell encourages me to concentrate on this topic and hope to discover something interesting and worth further study.

II. Technical background

❖ *Basic mechanism*

The multi-junction is made of stacked P-N junctions, the most basic building blocks of all crystalline Solar cells. The varies bandgap existed in all kind of semiconductors enable the possibility of photovoltaic devices. The mechanism of such process works in the way that valence electrons receive sufficient energy to overcome the bandgap, a conduction band electron is created, leaving behind a positively charged "hole" in the valence band as shown in figure 4. The bandgap Eg contains no allowed energy levels for electrons to occupy and is known as the "forbidden band".

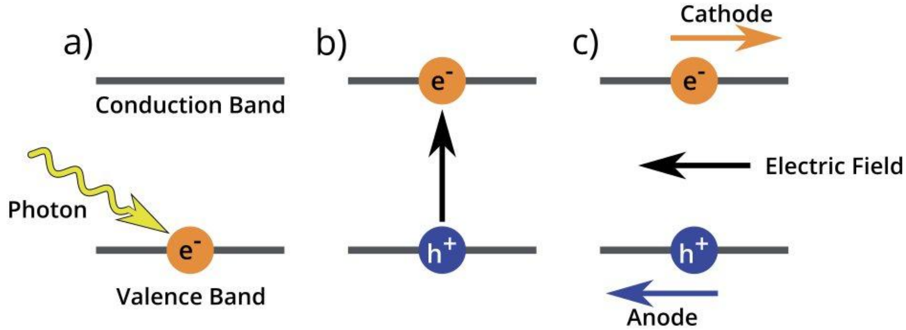

Figure 3: The photon absorption mechanism

The main focus of design parameters for solar cells are the optimum band gap and shortest minority carrier diffusion length. The former determines at which point in the solar spectrum the semiconductor starts absorbing light, the latter determine how far minority carriers diffuse before recombining. The ultimate goal of a solar cell design is to have the photo generated minority carriers enter external circuit and do work before they recombine.

❖ *Physical Models for solar cells*

There are two most essential models of a single junction solar cell: the diode model and double diode model which intends to include both the effects of carrier recombination in the bulk material and at surfaces through n = 1 behavior and in the junction through n = 2 behavior.

The fundamental formulas of solar cells revealed the relationship between current density and bias voltage:

$$\mathrm{J(V)} = \mathrm{J_{pho}} - \mathrm{J_0} * (\mathrm{e}^{\frac{q(V+JAR_S)}{k_b nT}} - 1) - \frac{V+JAR_S}{AR_{SH}}$$

Where J_{pho} is the generated light current density (for most cases $J_{\text{pho}} = J_{SC}$ short circuit current density) and the second term represents ideal diode behavior when the ideality factor n = 1. It is clear that the solar cell behaves like a current source connected parallel to an ideal diode. And it would make sense that solar cells, no matter how many junctions, are all operating in the fourth quadrant.

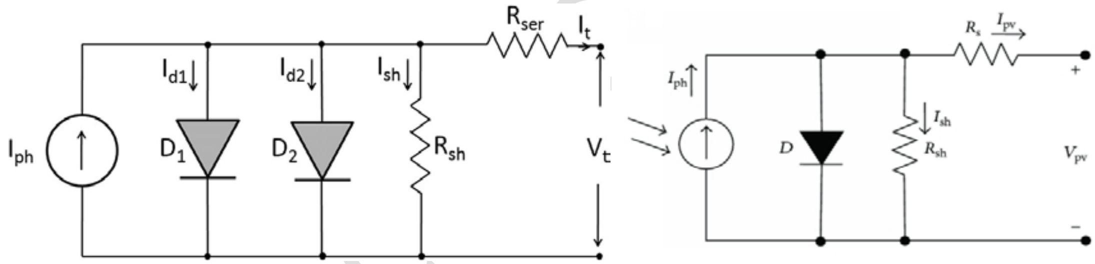

Figure 4: Equivalent circuit of Single Diode and double Dual Diode solar cells

Moreover, the double diode model of solar cell reveals a similar relation between the current density and voltage, but more accurate:

$$\mathrm{J(V)} = J_{pho} - J_{01} * (e^{\frac{q(V+JAR_S)}{k_b T}} - 1) - J_{02} * (e^{\frac{q(V+JAR_S)}{2k_b T}} - 1) - \frac{V+JAR_S}{AR_{SH}}$$

Below is an example I-V curve adopted from the datasheet of a commercialized product, similar predictions are expected.

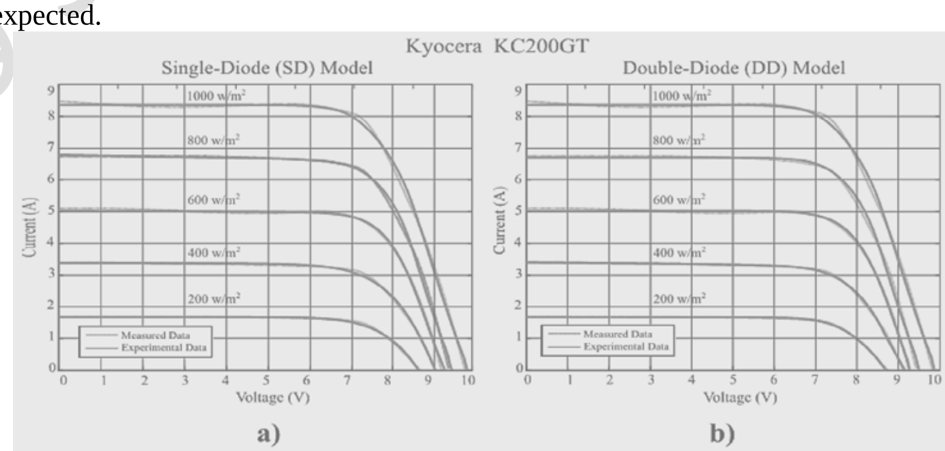

Figure 5:Estimated I-V characteristics curves at different irradiance levels (200, 400, 600, 800 and 1000 W/m2) and fixed cell temperature (Tc=33 °C) for an individual cell from a Kyocera KC200GT Solar Panel. (a) SD model and (b) DD model. [3]

Both the modeling and fabrication of a simple single junction diode are straightforward, a PIN diode, and the induced excess carriers in intrinsic region are swiped out through the internal electric field of PN junction.

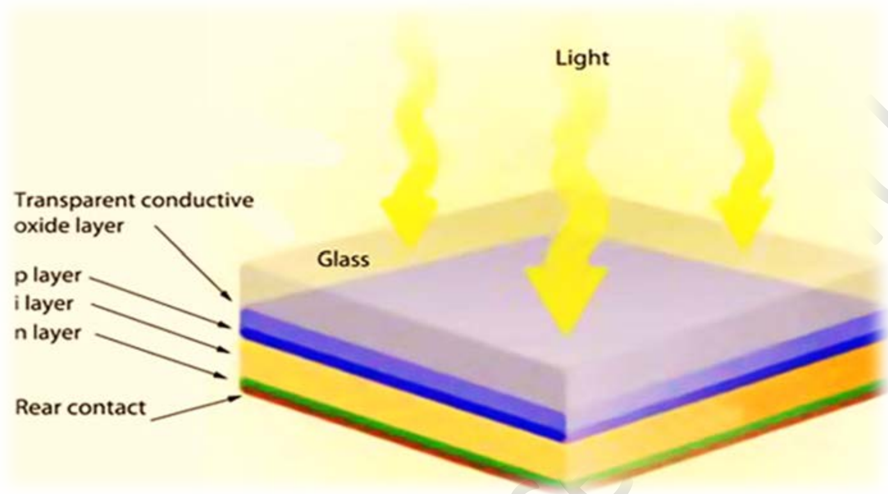

Figure 6: Regular PIN Junction

❖ *Direct & Indirect*

The Relation between the different bandgap types of materials and its characteristic feature associated with in solar cell industry was mentioned a lot, but not go into detail on how semiconductor devices are optimized for their particular function. E-k space is essential to understand this, given that it depends on the direct and indirect nature of the semiconductor.

Direct band gap materials have strong optical transitions between the valence and conduction band. However indirect materials have fairly weak optical transitions. This is because absorption and emission of a photon must occur with the simultaneous absorption or emission of a phonon (thus conversing momentum).

Comparing GaAs (direct material) solar cell to a Si (indirect material), it is clear that Silicon cells are much thicker: on the order of hundreds of microns, aiming to balancing its weaker absorption coefficient. Moreover, Silicon is a poor absorber of light, simply having a greater thickness meaning absorption of nearly all of incoming photons.

❖ *Modeling and Simulation of Multi-Junction Solar Cells*

However, for multijunction solar cell, everything is much more complicated. The situation of analyzing and understanding trades-offs beneath the multi-junction solar cell performance is extremely complicated. For instance, the triple junction showed in Figure 1 clearly revealed how complicated the structure could be. Each junction will have a BSF, emitter, base, window and even an extra tunnel junction. The total amount of layers is calculated as below:

Table 2: # of junctions VS total layers

The # of junctions	BSF Layer	Base	Emitter	Window	Tunnel Junction	Buffer	Total
2	2	2	2	2	2	0	10
3	3	3	3	3	4	0	16
4	4	4	4	4	6	0	22
5	5	5	5	5	8	4	32
6	6	6	6	6	10	6	40

It is clear that the degree of freedom of a system is incredibly huge. For instance, a five junction will have 30 layers as calculated above, and every layer has a determined thickness, doping, and material composition. Assuming that each layer has six possibilities for each parameter (which is the minimal: for doping material and thickness), then there will be 6*6*6 = 216 outcomes in total. Then thirty layers will result in total amount of 216^30 = 1.08E70 combinations. In research field, there is a method called genetic algorithm.

❖ *Genetic Algorithms [6]*

Genetic algorithms utilize a survival-of-the–fittest principle as a meta heuristic to optimize different solar cell parameters based on random generation of initial parameters. It is an iterative, stochastic nonlinear process that does not rely on strict mathematical formulation [19]. With regard to solar cells, parameters such as doping concentration and layer thickness is seen as genes in a “chromosome”.

The following parent chromosome execution in the simulation environment that defines the inferior solutions and best solutions in the design. Values that are seen as providing the best output from prior generations are kept, while inferior values are left behind. Bates utilized four binary bits to describe each of the parameters, leading to 16 different values that each parameter could take [2]. An example chromosome utilized by Bates in shown in the figure below:

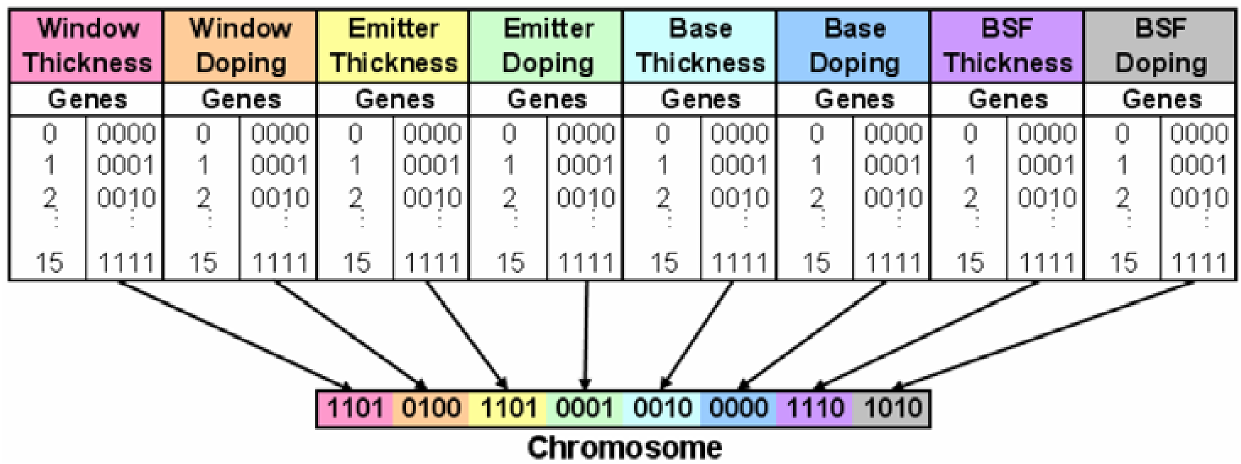

Figure 7: Genetic algorithm [6]

In this case, the variable is just the doping and thickness for each layer, and the tunnel junction is excluded in the optimization. Through this special chromosome coding, it is much more efficiency to try out all the possible combinations of all the layers.

However, this is a potentially useful but impractical technique for me to practice, I spent the whole week to fine tune every parameter to make the newton par solver of Apsys finally converge, after the successful convergence some modifications are done, but each simulation will still consume 20 mins. Moreover, the genetic algorithm would be an extra effort to implement, and the Crosslight software does not apparently support that. Therefore, it is not possible for me to figure out the best parameter set that will maximize the performance. I will develop and take advantage of this algorithm in the near future to figure out the best five junction solar cell parameter set.

❖ *Lattice constant & lattice match*

The final design issue to address would be the lattice match condition of different materials.

Perfect crystals are arrays of regularly spaced atoms, but atomic spacing differs among compounds. Failure to match the atoms in successive layers can produce defects in the crystal, which degrade its optical, electronic, or mechanical properties.

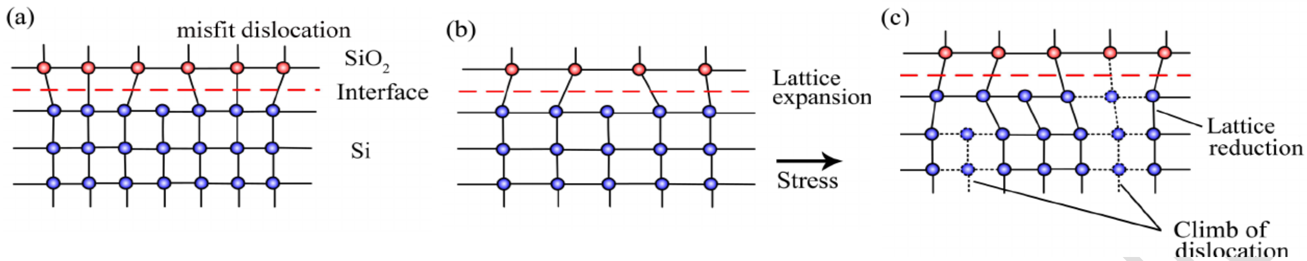

[8] Figure 8:Schematically showing the deformation processes of silica / silicon system due to external stress, (a) misfit dislocations exist at interface, (b) expansion of silicon lattice due to tensile stress, and (c) stress relaxation and lattice reduction due to climb of dislocation in the substrate.

Therefore, it is important to select a material system, containing five compound materials that are lattice matched to each other. Generally, materials that are lattice matched to GaAs is preferred in many multijunction solar cells.

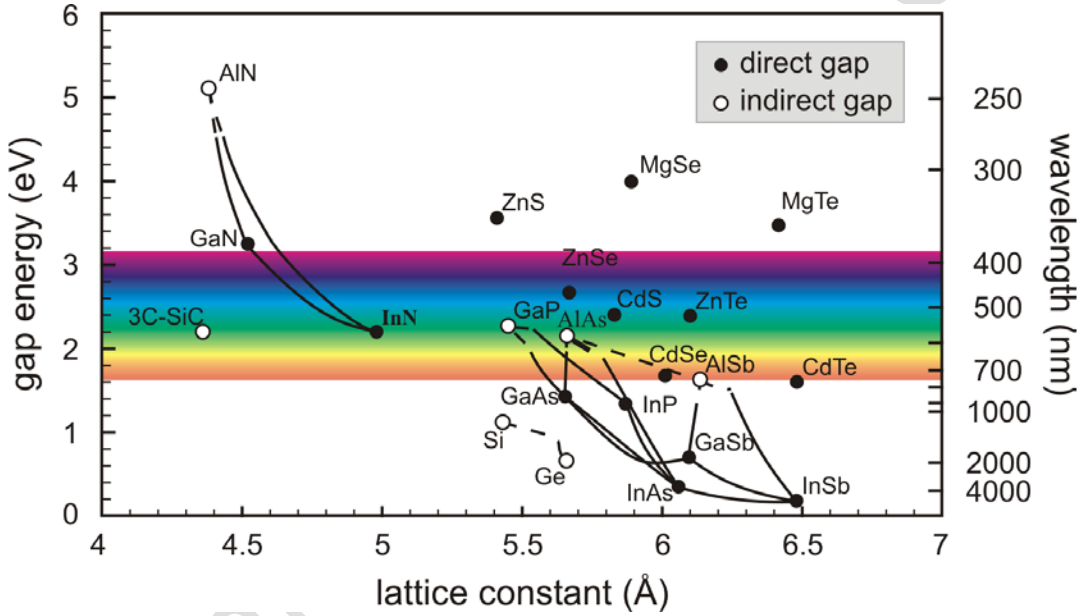

Figure 9:Material Systems

❖ *Fill factor and maximum power [12]*

The short-circuit current and the open-circuit voltage are the maximum current and voltage respectively from a solar cell. However, at both of these operating points, the power from the solar cell is zero. Fill factor is a parameter which, in conjunction with Voc and Isc, determines the maximum power from a solar cell. The FF is defined as the ratio of the maximum power from the solar cell to the product of Voc and Isc. As FF is a measure of the "squareness" of the IV curve, a solar cell with a higher voltage has a larger possible FF since the "rounded" portion of the IV curve takes up less area. The maximum theoretical FF from a solar cell can be determined by differentiating the power from a solar cell with respect to voltage and finding where this is equal to zero.

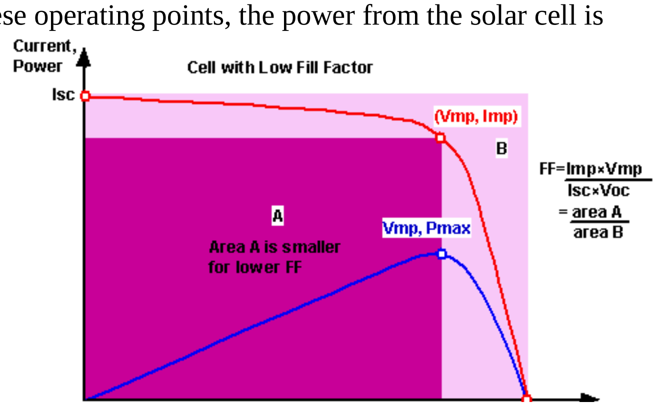

Figure 10: Fill factor explanation

III. The starting point: Double BSF Layer InGaP/GaAs DJ solar cell

In order to get familiar with Crosslight software and understand the basic workflow, I started from modeling a relatively simple but robust InGaP/GaAs dual junction solar cell regarding its tremendously high efficiency of 34.52% under AM 1.5 standard test condition, and 39.15% under 1000 suns. And the material parameters are provided in the original table of literature:

Table 3: The material properties of Dual junction solar cell [11]

Material	**GaAs**	**InGaP**	**InAlGaP**
Band gap Eg (eV) @300 K	1.42	1.9	2.3
Lattice constant α (Å)	5.65	5.65	5.65
Permittivity (∈ s/∈ o)	13.1	11.6	11.7
Affinity (eV)	4.07	4.16	4.2
Heavy e− effective mass (m_e/m_0)*	0.063	3	2.85
Heavy h + effective mass (m_h/m_0)*	0.5	0.64	0.64
e− mobility MUN ($cm^2/V \times s$)	8800	1945	2150
h + mobility MUP ($cm^2/V \times s$)	400	141	141
e− density of states N_C (cm^{-3})	4.7e+17	1.30e+20	1.20e+20
h + density of states N_V (cm^{-3})	7.0e+18	1.28e+19	1.28e+19
Lifetime (el) (s)	1.00e−09	1.00e−09	1.00e−09
Lifetime (ho) (s)	2.00e−08	1.00e−09	1.00e−09
n_i (per cc)	2.12e+06	7.43e+04	1
V_{satn} (cm/s)	7.70e+06	1.00e+06	1.00e+06
V_{satp} (cm/s)	7.70e+06	1.00e+06	1.00e+06

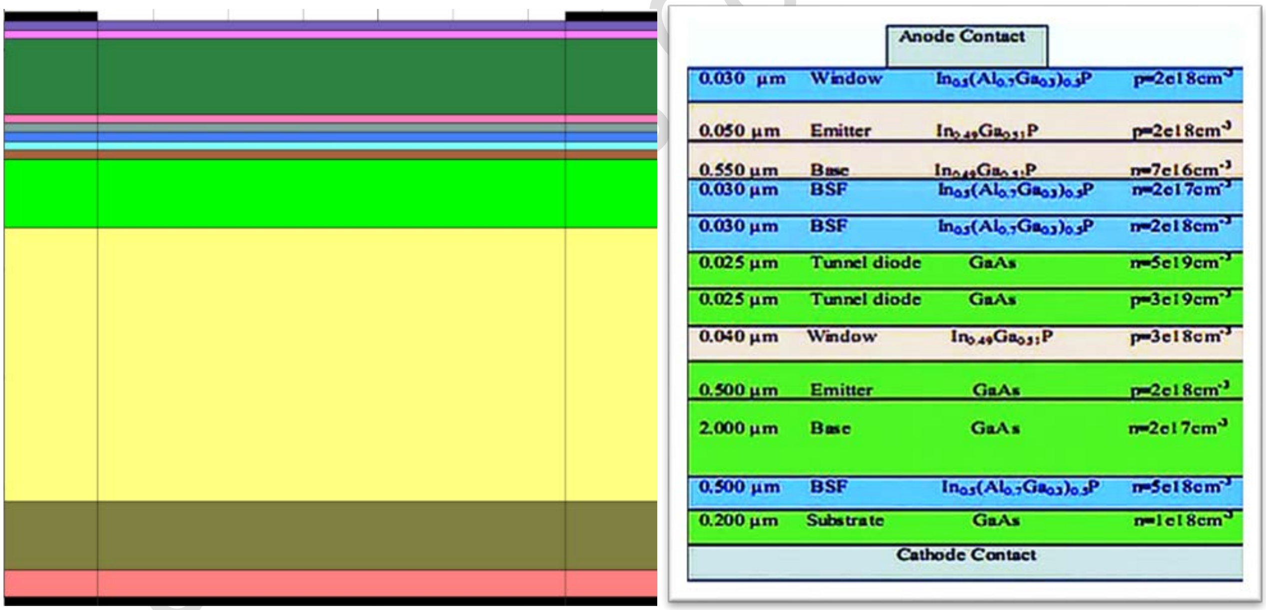

Figure 11: Base design of Dual junction solar cell and Structure in Crosslight [11]

The modeling is quite straightforward in this case, and only the solution file is pretty difficult to write regarding the issue of convergence. Moreover, the index files in Crosslight are unable to describe the complex refractive index of each layer, making the convergence impossible. Therefore, I imported the refractive index from [4] for every material I used, and the solution finally converged. The I-V curve and results are shown below:

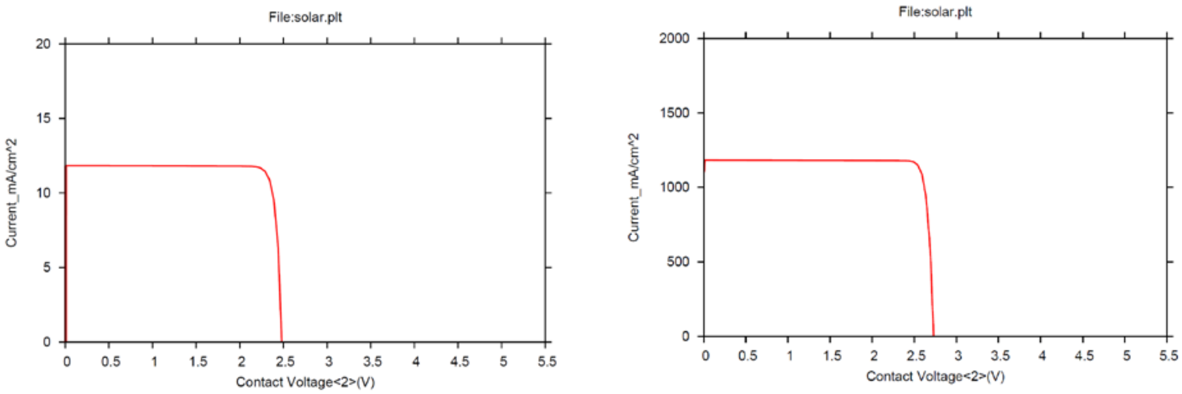

Figure 12: I-V Curve: a)under 1 Sun. b) under 100 sun.

In order to compare the Crosslight simulation result with a known structure, I tuned every parameter including the refractive index file exactly the same as reported in the article [4], and

Condition	Vmax	Jmax	Voc	Jsc (mA/cm^2)	Pmax	eff	FF
1 sun	2.275V	11.5099	2.48V	11.8291	26.1826	26.1%	0.893
Reported 1 sun			2.66V	17.33		34.52%	0.8867
100 sun	2.526V	11569.890	2.729V	1183.840	2922.67	29.2%	0.905

In conclusion, the result in the reported simulation on Silvaco has about (34.52-26.1)/26.1 = 32.2% more efficiency than the result in Crosslight. And the major difference is the short circuit current, since the open circuit voltage is nearly the same. Therefore, it is acceptable that Crosslight will underestimate the current of 5J multijunction solar cell as well.

IV. The model baseline: FRAUNHOFER ISE 5-J CELL [5]

According to the Fraunhofer Institute for Solar Energy Systems, new Multijunction solar cell structures with over five junctions have been developed to further improve the radiation resistance. The structure consists of AlGaInP, GaInP, AlGaInAs, GaInAs and Ge active PN junctions.

Figure 13: 5-junction solar cell structure with composition, layer thickness and bandgap of the different PN junctions. [5]

	Composition	d	Eg
J1	(Al0.3Ga0.7)InP	175 nm	2.14 eV
J2	Ga0.5In0.5P	570 nm	1.88 eV
J3	(Al0.1Ga0.9)In$_0$As	415 nm	1.51 eV
J4	Ga0.99In0.01As	1105 nm	1.41 eV
J5	active Ge	150 µm	0.67 eV

However, the increasing number of junctions have imposed significant difficulties for fabrication. Below is a contour plot of efficiency provided by the Fraunhofer Institute. Although it is observed that the maximum efficiency of 43.5 % is achieved for a top cell with Eg = 2.45 eV and a 3rd subcell with Eg = 1.65 eV, it is relatively hard to achieve the theoretical limit, and the experimental efficiency is about 22%.

Moreover, according to the result of figure 13, it is stated that top junction of 2.4ev and middle junction of 1.65ev bandgap can maximize the efficiency. I tuned the top material into $(Al_{0.52}In_{0.48}P)_z(Ga_{0.51}In_{0.49}P)_{1-z}$,*[7]* where z = 0.5 in order to lattice match to GaAs [7]. And the bandgap is given by:

$$Eg = 2.007(1 - z) + 2.691z - 0.18z(1 - z) \text{ eV}$$

When z = 0.5, Eg = 2.304ev, and it is confirmed in the band diagram below. The improvement in efficiency is about 1.5% by only changing the material composition of the top cell.

To prevent the convergence issue occurred in the Crosslight, the structure is designed as Table 2 illustrated, and the bandgap of Junction three is tuned to 1.61ev and In component is completely removed. The advantages of this modification are efficiency maximization and ensurance of lattice match to GaAs.

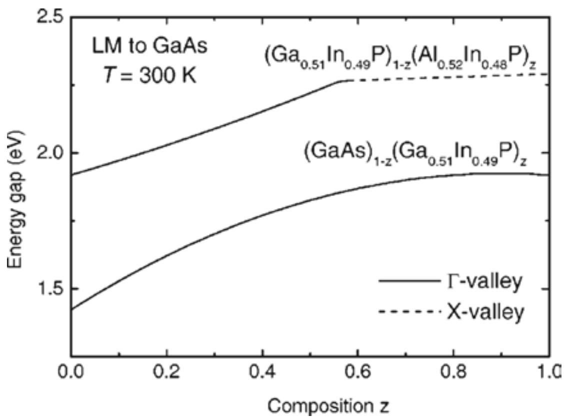

Figure 14: Lowest energy gaps as a function of composition of two quaternaries.

Figure 15: Thermodynamic limit of cell efficiency Vs Bandgap

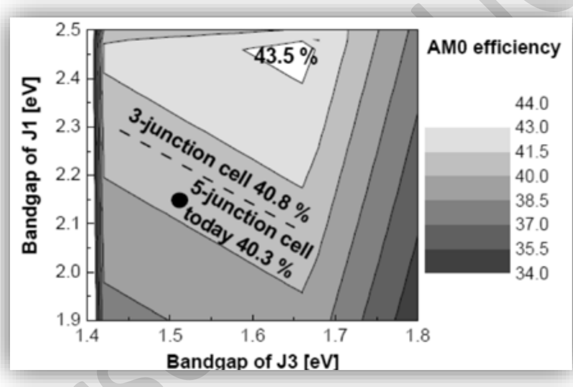

Table 4: cell modeling the Dimroth et al. five-junction solar cell

Ohmic Contact	Top Contact			
AlInP	Window	n+	0.01	2E18 cm'1
$(Al_{0.3}Ga_{0.7})_{0.52}In_{0.48}P$	Emitter	n+	0.02	2E18 cm'3
	Base	P+	0.125	1.5E17 cm'3
	BSF	P+	0.01	2E18 cm'3
AlInP	Buffer	P+	0.01	1E18 cm'1
$Al_{0.1}Ga_{0.9}As$	Emitter	P+	0.015	8E18 cm'1
$Ga_{0.52}In_{0.48}P$	Base	n+	0.015	1E19 cm'3
AlInP	Window	n+	0.01	2E18 cm'3
$Ga_{0.52}In_{0.48}P$	Emitter	n+	0.07	2E18 cm'3
	Base	P+	0.5	1.5E17 cm'3
	BSF	P+	0.01	2E18 cm'3
AlInP	Buffer	P+	0.1	1E17 cm'3
$Al_{0.1}Ga_{0.9}As$	Emitter	P+	0.015	8E18 cm'3
$Ga_{0.52}In_{0.48}P$	Base	n+	0.015	1E19 cm'3
GaAs	Window	n+	0.03	2E18 cm'3
$Al_{0.1}Ga_{0.9}As$	Emitter	n+	0.03	2E18 cm'3
	Base	P+	0.275	1.5E17 cm'3
	BSF	P+	0.03	2E18 cm'3
GaAs	Buffer	P+	0.03	1E18 cm'3
$Al_{0.1}Ga_{0.9}As$	Emitter	P+	0.015	8E18 cm'3
$Ga_{0.52}In_{0.48}P$	Base	n+	0.015	1E19 cm'3
GaAs	Window	n+	0.03	2E18 cm'3
$Ga_{0.99}In_{0.01}As$	Emitter	n+	0.05	2E18 cm'3
	Base	P+	0.965	1.5E17 cm'3
	BSF	P+	0.03	2E18 cm'3
GaAs	Buffer	P+	0.03	2E18 cm'3
$Al_{0.1}Ga_{0.9}As$	Emitter	P+	0.015	8E18 cm'3
$Ga_{0.99}In_{0.01}As$	Base	n+	0.015	1E19 cm'3
GaAs	Window	n+	0.03	2E18 cm'3
Ge	Emitter	n+	0.01	2E18 cm'3
	Substrate	P+	149.96	1.5E17 cm'3
Ohmic Contact	Anode			

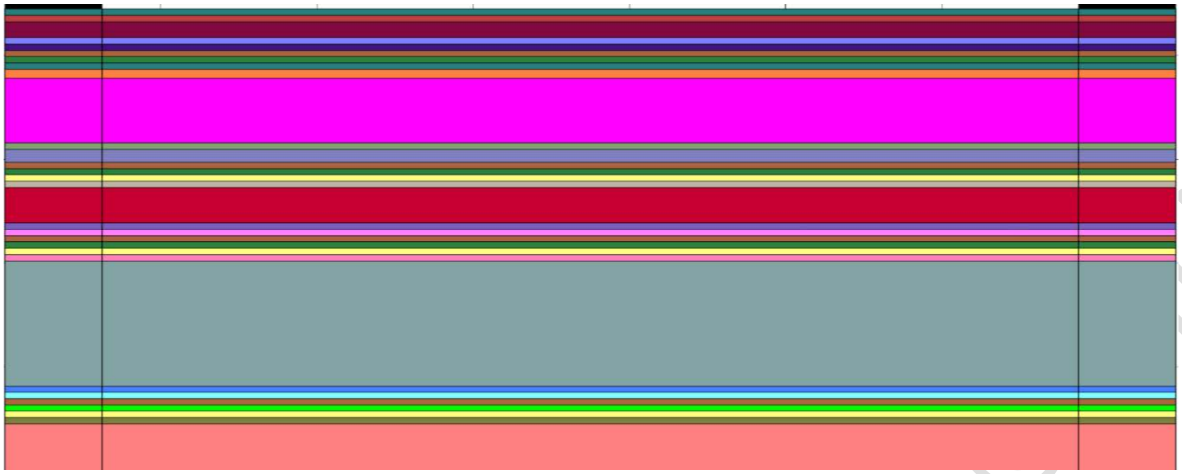

Figure 16: The Baseline Structure of five junction solar cell

❖ *Baseline Results:*

After a week's tuning and prototyping, the structure as listed above finally worked and the solver eventually converged. Although the output current density is much lower than I expected, the overall result besides current density is reasonable. The test condition is standard AM1.5.

Condition	Vmax	Jmax (mA/cm^2)	Voc	Jsc (mA/cm^2)	Pmax	eff	FF
1 sun	4.907V	3.1324	5.28V	3.3164	15.371	15.327%	0.893
Reported			5.26 V	7.5		20-24%	Roughly0.9

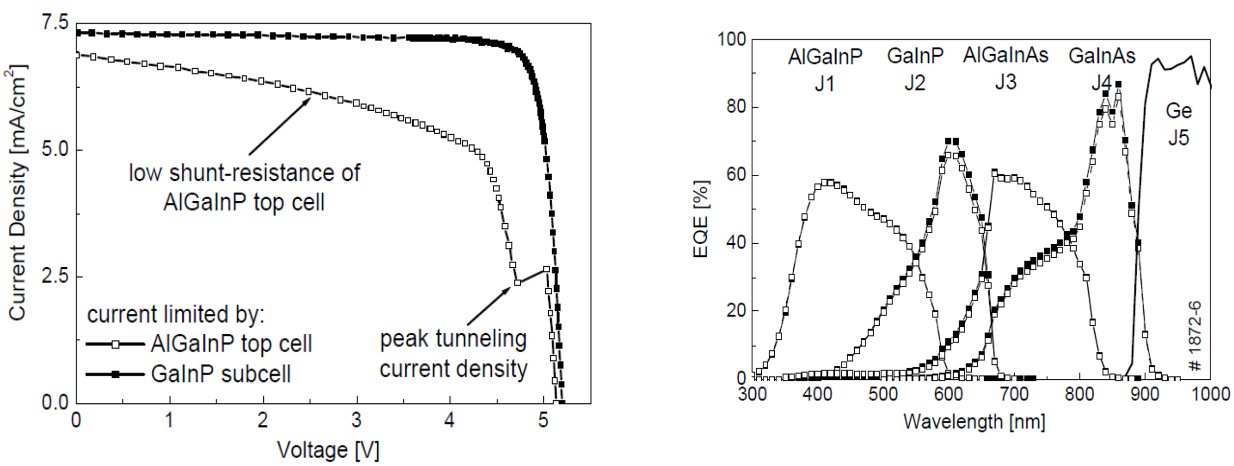

Figure 17:a)Reported IV-characteristics of two 5-junction solar cells.b)Reported External Quantum Efficiency (EQE) of the 5-junction solar cell [5]

Therefore, comparing to the experimental result, every parameter besides short circuit current is quiet close, especially the open circuit voltage. And the efficiency of 15.3% is much lower than expected range of 20%-24% because of the much lower short circuit current. Therefore, it is expected that current matching issue existed in present design what causing the issue.

❖ *Parameter optimization*

Although I am interested in the genetic algorithm, but it is too hard for me to implement for parameter optimization. Based on previous result, the Current matching issue is more likely to be account for the loss of efficiency and current density. Therefore, I will only adjust the base thickness of each junction to find out the best parameter set, and let other parameters fixed.

Each simulation takes more than fifteen minutes to complete, so choose a nice point to start is crucial to successfully performing the optimization. Observing that the issue is mainly caused by relatively low current density, I will only change the thickness of each absorbing layer, the base thickness to account for a current matching. Because the baseline model is already well organized, the primary goal would be find out a local maximum start from the baseline thickness and stick to it, until a maximum efficiency is achieved.

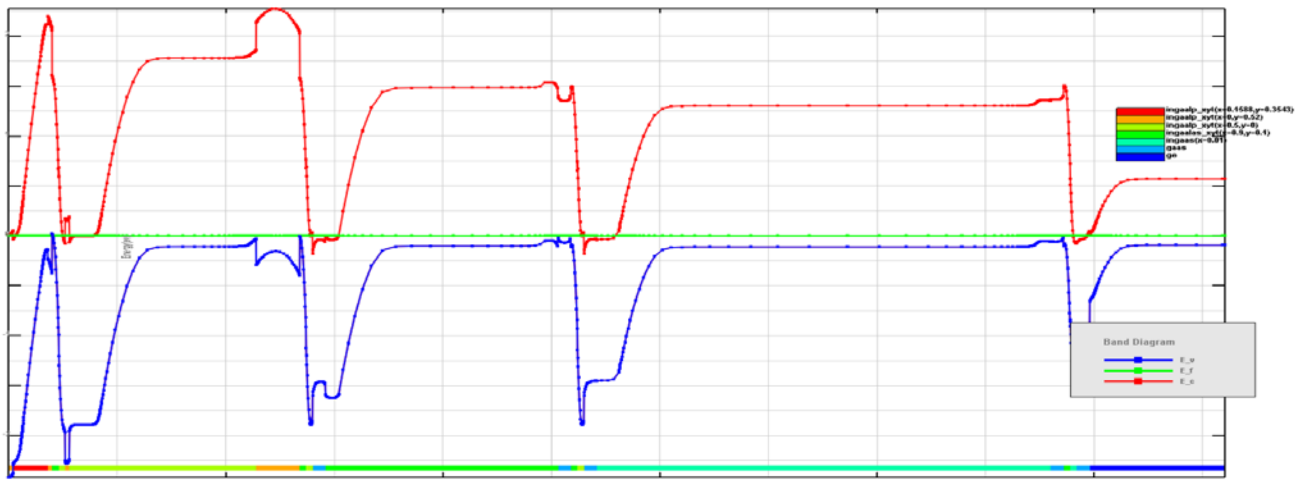

Figure 18: Band Diagram of 5-J Multijunction Solar Cell at equilibrium

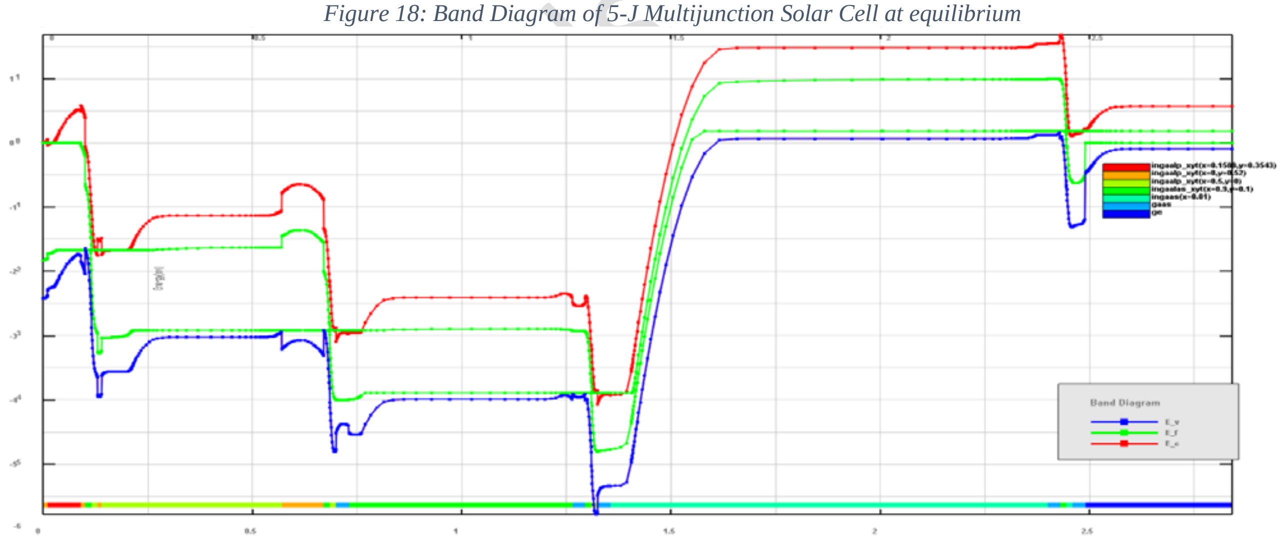

Figure 19: Band diagram under illumination

After another week's tuning and simulation, the dependence of efficiency on base thickness of each junction is fully explored. It turns out that the third base affect the efficiency most significantly, changing base 3 thickness only yield 3% more efficiency improvement after changing the material, reaching 18%. Moreover, the short circuit current density increases with the thickness of base 3 following the same trend of efficiency increasing. And the fill factor reaches a local maximum at b3 = 0.475um.

Therefore, it is reasonable to try the combination of best performing base thickness out of baseline model to achieve the maximum efficiency. Also, the modified Base 1 with relatively thinner window at b1 = 0.04um is not better than having b1 = 0.05um. From the result of figure 19, my next generation model will fix the b1=0.05, b2= 0.35um, b3=0.475um, because those junction thickness are located in local maximum according to graphs below, whereas the b4 is not reaching a local maximum.

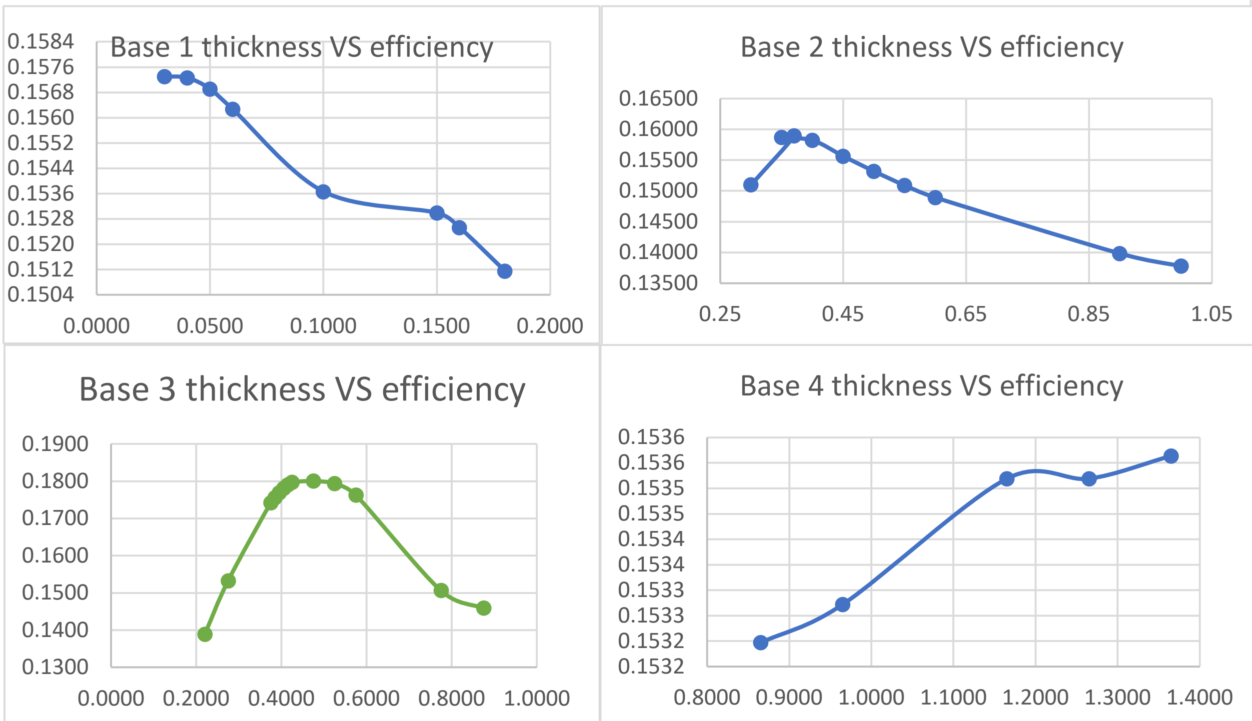

Figure 21: Baseline model with one base thickness varied Vs Efficiency

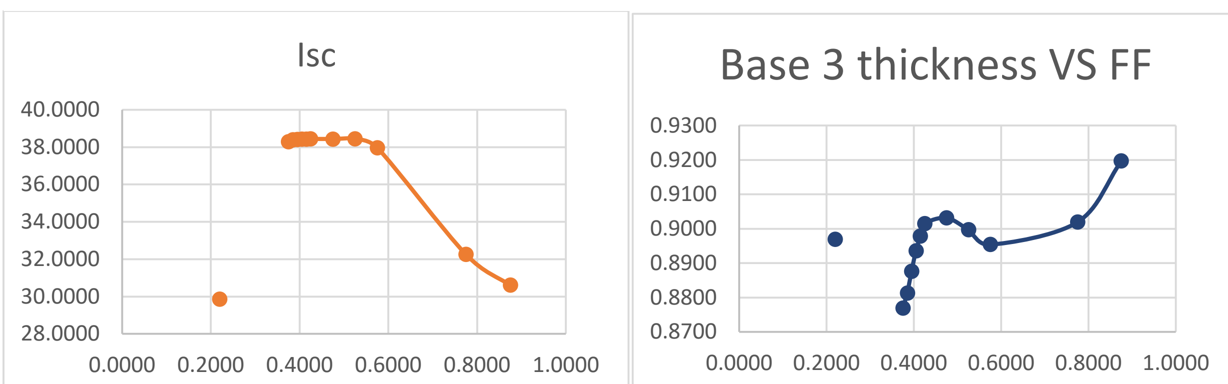

Figure 20: Short circuit current density & FF Vs base 3 thickness

- ***Generation 2: b1=0.05, b2= 0.35um, b3=0.475um***

It is obvious that as thickness of b4 increases, the efficiency increases and saturates as b4 is above 1.7um. The efficiency of the cell reaching the peak of 21.98% as b4 =1.96um.

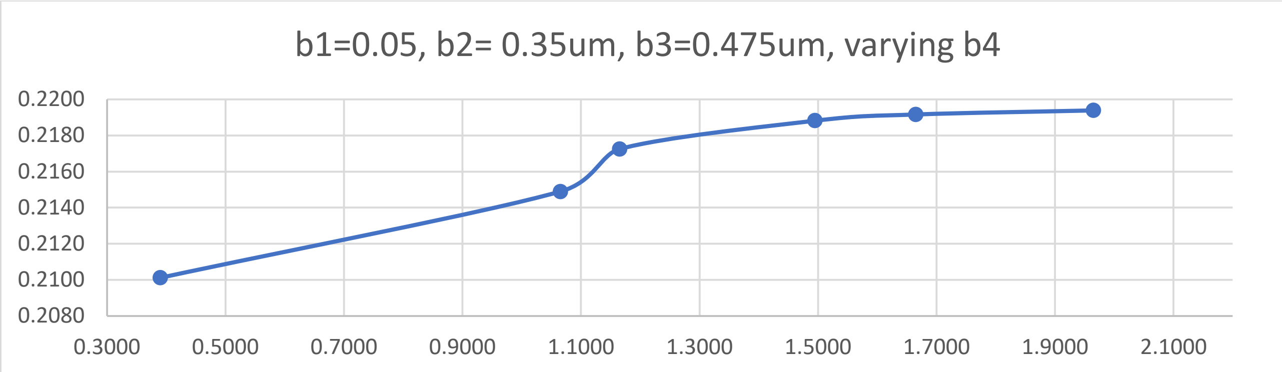

Figure 22: Generation 2, varying b4

CONDITION	V_{MAX}	J_{MAX} (MA/CM^2)	VOC	JSC (MA/CM^2)	P_{MAX}	EFFICIENCY	FF
1 SUN (BEST CASE)	5.07567 V	4.33497	5.28V	4.4204	22.029	21.939 %	0.943
1 SUN(BASE)	4.907V	3.1324	5.28V	3.3164	15.371	15.327%	0.893
REPORTED			5.26V	7.5		20-24%	0.85

Figure 23： Improvements of modification

V. Conclusion

The simulation of five junctions solar cell turns out to be much more difficult as I expected. The design of each window, base, emitter, BSF and buffer layer consumed me a lot of time. Tunnel junction is another issue I need to carefully treat with. The tunnel junction is an ultrathin (30nm), highly doped (10^19cm-3) PN junction that aims to transfer photocurrent generated in each junction. Depending on the section of spectrum that is absorbed in each layer, every sublayer absorb whatever left in the solar spectrum and generate photocurrent. The current matching of different layers and high efficiency collection in each layer is a difficult technical problem. The current density plot of final design shows that only at the edge of the cell, where the electrodes locate, has relatively high current density between each junction. In central regions the current density is nearly uniform as figure 23 shows. Besides, all five base thicknesses are tuned to be a local maximum, revealing that the base thickness of all five junctions are already at optimum level. The matching of an efficiency of 21.98% is also expected as experimental values in [5], which are between 20-24%. Further modification would rely on the genetic algorithm introduced previously, capable of tuning the doping, material composition, thickness, of all thirty layers to achieve the ultimate optimum design of the given material system.

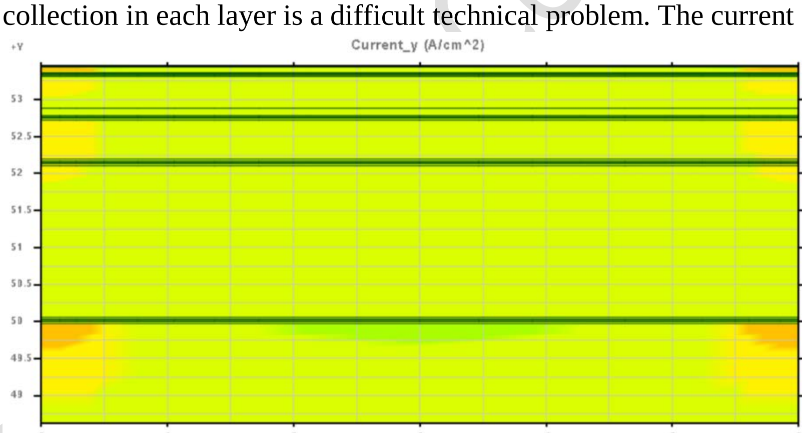

Figure 24: current density Distribution

The improvement of optimizing base thickness by finding local maximum efficiency of each layer works out perfectly. The overall efficiency increases from 15.327% to 21.98%, a 43.4% increase in efficiency, which fits the experimental value very well. And the short circuit current density improved from 3.3164 mA/cm^2 to 4.4204 mA/cm^2, about 33.28% increases. The increasing in short circuit current contribute the most to the increase of efficiency.

Moreover, the material system implementing the five junction solar cell is not the best choice that maximize the efficiency. According to source [5], this design is initially used to reduce radiation degradation of the solar cell. So I suppose that any further improvements would rely on selecting different material systems.

Reference

1. B Honsberg, C & Barnett, Allen. (2005). Paths to ultra-high efficiency (> 50% efficient) photovoltaic devices.
2. P. Michalopoulos, "A novel approach for the development and optimization of state-of-the-art photovoltaic devices using Silvaco," M.S. thesis, Dept. of Elec. and Comp. Engr., Naval Postgraduate School, Monterey, CA, 2002.
3. Kyocera Corporation, KC200GT, PHOTOVOLTAIC MODULE, https://www.kyocerasolar.com/dealers/product-center/archives/spec-sheets/KC200GT.pdf
4. M. N. Polyanskiy, "Refractive index database," https://refractiveindex.info . Accessed on 2018-04-21
5. F. Dimroth, C. Baur, A. W. Bett, W. Kostler, M. Meusel and G. Strobl, "Thin 5-junction solar cells with improved radiation hardness," in *4th World Conference on Photovoltaic Energy Conversion*, Waikoloa, HI, 2006, pp. 1777–1780.
6. A. D. Bates, "Novel optimization techniques for multi-junction solar cell design using Silvaco ATLAS," M.S. thesis, Dept. of Elec. and Comp. Engr., Naval Postgraduate School, Monterey, CA, 2004.
7. I. Vurgaftman and J. R. Meyer, Band parameters for III–V compound semiconductors and their alloys, Journal of Applied Physics 89, 5815 (2001), https://doi.org/10.1063/1.1368156
8. hang, Yanghang, Xian-Chengu, Shan-Tung 015/09/0197105IP Advance soupled mechanical-oxidation modeling during silicon thermal oxidation process https://doi.org/0.1063/1.4930255
9. C. B. Honsberg, Paths to ultra-high efficiency (>50% efficient) photovoltaic devices, 20th European Photovoltaic Solar Energy Conference, 2005.
10. Kilway, Raymond J. Five-junction solar cell optimization using Silvaco ATLAS, II Monterey, California: Naval Postgraduate School
11. P.Nayak, J.P.Dutta, G.P.Mishra, Efficient InGaP/GaAs DJ solar cell with double back surface field layer, Engineering Science and Technology, an International Journal, Volume 18, Issue 3, September 2015, Pages 325-335
12. M. A. Green, "Solar cell fill factors: General graph and empirical expressions", Solid-State Electronics, vol. 24, pp. 788 - 789, 1981.